Original Research Paper

Targeting the resolution pathway of inflammation using Ac2–26 peptide-loaded PEGylated lipid nanoparticles for the remission of rheumatoid arthritis

Xianyan Qin[a], Liming He[a], Donghao Fan[a], Wenlang Liang[a], Qin Wang[a,], Jiyu Fang[b,*]*

[a] *Key Laboratory of Advanced Technologies of Materials, Ministry of Education and School of Materials Science and Engineering, Southwest Jiaotong University, Chengdu 610031, China*

[b] *Advanced Materials Processing and Analysis Center and Department of Materials Science and Engineering, University of Central Florida, Florida 32816, United State*

ARTICLE INFO

ABSTRACT

Rheumatoid arthritis (RA) is a common autoimmune disease characterized by joint inflammation and immune dysfunction. Although various therapeutic approaches have been utilized for the treatment of RA in clinical applications, the low responsiveness of RA patients and undesired systemic toxicity are still unresolved problems. Targeting the resolution pathway of inflammation with pro-resolving mediators would evoke the protective actions of patient for combating the inflammation. Ac2–26, a 25-amino acid peptide derived from Annexin A (a pro-resolving mediator), has shown good efficacy in the treatment of inflammatory disorders. However, the low bioavailability of Ac2–26 peptides hinders their efficacy *in vivo*. In this paper, we formed PEGylated lipid nanoparticles (LDNPs) by the co-assembly of L-ascorbyl palmitate (L-AP) and N-(carbonyl methoxypolyethylene glycol-2000)-1,2-distearoyl-sn–glycero-3-phosphoethanolamine (DSPE-PEG$_{2k}$) to encapsulate and deliver Ac2–26 peptides to the arthritic rats. They showed good stability and biocompatibility. After being intravenously administrated, Ac2–26 peptide-loaded PEGylated lipid nanoparticles (ADNPs) showed the prolonged *in vivo* circulation time and enhanced accumulation in inflamed sites. *In vivo* therapeutic evaluations revealed that ADNPs could attenuate synovial inflammation and improve joint pathology. Therefore, the pro-resolving therapeutic strategy using ADNPs is effective in RA treatment.

* Corresponding authors.
E-mail addresses: wangqin666@swjtu.edu.cn (Q. Wang), jiyu.fang@ucf.edu (J.Y. Fang).
Peer review under responsibility of Shenyang Pharmaceutical University.

1. Introduction

Rheumatoid arthritis (RA) is one of the most widespread autoimmune diseases, which affects approximately 1% of the global population [1]. RA is usually characterized by the infiltration of inflammatory cells, the destruction of joints and the activation of autoimmune systems [2,3]. Particularly, the rapid proliferation and activation of T cells and B cells in inflamed joints break the balance between the host immune tolerance and immune homeostasis, leading to the attack of immune systems to own tissues persistently [4]. There are numerous anti-inflammatory therapeutic agents available in clinical applications. Most of them are based on immunosuppression or blocking certain inflammatory signaling pathways. However, the current therapies are often undesirable [5,6]. For example, clinical studies showed that approximately 50% of RA patients show low responsiveness [7]. Moreover, the treatment of RA usually requires a long-term therapy, which is often associated with systemic comorbidities [8].

It is generally considered that the onset of inflammatory diseases is accompanied by a pro-inflammatory phase. The remission of diseases is often followed by a resolution phase [9]. In the resolution phase, a variety of endogenous pro-resolving mediators would be produced. They could promote inflammation remission, tissue repair and restoration of immune homeostasis [10]. In RA, the deficiency of the resolution mechanism commonly leads to a prolonged disease course, consequently resulting in the chronicity of diseases and widespread complications [11]. Therefore, remodeling the resolution function by replenishing sufficient pro-resolving mediators might provide a potential avenue for the effective treatment of RA [12]. Compared with conventional treatments, the pro-resolving therapeutic strategy has several advantages: (1) motivate the protective action of patient's own tissues to combat the inflammatory infiltration and tissue damage; (2) balance the level of T helper17 (Th17) and regulatory T (T_{reg}) cells to restore the immune homeostasis; and (3) reduce the burden of adverse effects [13,14].

So far, the pro-resolving mediators discovered are basically endogenous molecules, including autacoids (such as adenosine, lipoxin A4 and maresin 1), proteins (such as annexin A1 and galectin-1) and polypeptides (such as αMSH) [7]. Among them, annexin A1 is a potent pro-resolving mediator, which would facilitate inflammation resolution and tissue repair via binding to the FPR2/ALX receptors [15]. However, there are various physiological barriers in the delivery of the protein drug, such as the degradation of multiple enzymes, the inability to transport across the membranes and the activation of excessive immune response in vivo. Currently, the pro-resolving mediators used in preclinical studies of chronic inflammatory diseases are mainly purified from the extracts of endogenous substances [16]. The purification process of pro-resolving mediators is complicated and expensive. In addition, the total synthesis of pro-resolving mediators would also face huge challenges such as high cost and low yield.

Ac2–26 is a mimetic peptide of annexin A1, which can be formed via solid-phase synthesis. Due to its low molecular weight and simple structure, Ac2–26 peptides possess better stability and lower immunogenicity than annexin A1 [17]. As a pro-resolving mediator, Ac2-26 peptide can inhibit the granulocyte trafficking and enhance the efferocytosis of macrophages in vivo [9,18], thus exerting the effect of inflammation resolution and tissue repair. Kamaly et al., found that Ac2–26 peptides could significantly reduce the recruitment of polymononuclear neutrophils and decrease the resolution interval in peritonitis mice [19]. Fredman et al., utilized Ac2–26 to stabilize advanced atherosclerotic lesions and promote inflammation resolution in atherosclerosis [20].

The application of peptides in vivo is often hindered by several barriers including enzymatic degradation and rapid elimination. In addition, Ac2–26 peptides are highly insoluble in aqueous solution. Nanocarriers have been extensively used as a feasible approach for improving the bioavailability of drugs by preventing them from enzyme degradation, extending their in vivo circulation and facilitating their passive delivery to inflamed joints [21,22]. It is worth noting that nanocarriers used in chronic inflammatory diseases should have good biocompatibility and not cause any immune activation or inflammatory responses [23].

N-(carbonyl methoxypolyethylene glycol-2000)−1,2-distearoyl-sn–glycero-3- phosphoethanolamine (DSPE-PEG$_{2k}$) has been approved by the Food and Drug Administration (FDA) for numerous medical applications [24,25]. It has been shown that PEGylated nanoparticles ensure the in vivo circulation time of therapeutic agents [26]. L-ascorbyl palmitate (L-AP), a potent antioxidant and scavenger of free radical, has been utilized as a nontoxic and efficient food additive [27]. In this paper, we prepared PEGylated lipid nanoparticles (LDNPs) by the co-assembly of L-AP and DSPE-PEG$_{2k}$, which can be used to encapsulate and deliver Ac2–26 peptides to arthritic joints. The physicochemical properties were systemically investigated. The in vivo pharmacokinetics and pharmacodynamic distribution behaviors were assessed in healthy rats and arthritic rats, respectively. In addition, the therapeutic efficacy and immune response of Ac2–26-loaded PEGylated lipid nanoparticles (ADNPs) were evaluated in arthritic rats. So far, the Ac2–26 peptide has never been applied in the treatment of RA. And there is no drug formulation designed aiming at the pro-resolving pathway to achieve the remission of RA. Therefore, our study would provide a new therapeutic approach for RA treatment.

2. Materials and methods

2.1. Materials

DSPE-PEG$_{2k}$ was obtained from Ponsure Biological (Shanghai, China). L-AP was purchased from Shanghai Aladdin Bio-Chem Technology Co., LTD (Shanghai, China). Cy5-NHS ester was purchased from Dalian Meilun Biotechnology Co., Ltd. (Dalian, China). Ac2–26 (AMVSEFLKQAWFIENEEQEYVQTVK) was obtained from Jier Biotech (Shanghai, China). Complete Freund's adjuvant (CFA) was provided by Chondrex, Inc.

(Washington DC, USA). Methanol, dimethyl sulfoxide (DMSO) and 1,2- propylene glycol were purchased from Kemiou (Tianjin, China). As for the analysis of flow cytometry, the antibodies BV605-CD3(clone 1F4), FITC–CD4 (clone OX35), PE-CD25 (clone OX39), APC-Foxp3 (clone FJK-16 s) and APC IL-17A (clone eBio18B7) were purchased from eBioscience (USA). Male SD rats were provided by the Dashuo experimental animal center (Chengdu, China). All animal studies were performed according to the recommendations in the U.S. National Institutes of Health Guide for the Care and Use of Laboratory and were approved by the Ethics committee of Southwest Jiaotong University.

2.2. Preparation of LDNPs and ADNPs

LDNPs were prepared via a thin film hydration method [28]. Firstly, L-AP (1 mg) and DSPE-PEG$_{2k}$ (5 mg) were dissolved in 4 ml methanol at the molar ratio of 1:1. The mixed solution was then added to a round bottom flask. After removing methanol by rotating evaporator under reduced pressure for 15 min at 50 °C, a thin film was formed in the bottom of the flask. LDNPs were formed after rehydrating the thin film in 2 ml deionized water at 50 °C. ADNPs were formed using the same procedure as mentioned above. Briefly, Ac2–26 (500 µg), L-AP (1 mg) and DSPE-PEG$_{2k}$ (5 mg) were completely dissolved in 4 ml methanol in a round-bottom flask. The ADNPs were formed after rehydrating the thin film with deionized water.

2.3. Characterization of LDNPs and ADNPs

The particle size and polydispersity index (PDI) of LDNPs and ADNPs were measured by dynamic light scattering (DLS) at 25 °C (Zetasizer Nano instrument, Anton Paar, Austria). The morphology of LDNPs and ADNPs were examined by a transmission electron microscope (TEM, JEOL TEM-1011, Japan). The absorption spectra of LDNPs and ADNPs were measured by Ultraviolet-visible (UV–vis) spectrophotometer (Agilent, Cary3500, USA).

2.4. Encapsulation efficiency and drug loading

The encapsulation efficiency (EE) and drug loading (DL) of ADNPs were investigated by ultrafiltration method [29]. Briefly, 1 ml ADNPs were added to an ultrafiltration tube (Millipore, MWCO100kD) and centrifuged at 2000 rpm for 15 min to separate free Ac2–26 and ADNPs. Then the subnatant of centrifugation samples was quantified with high-performance liquid chromatography (HPLC, Agilent 1260, USA). The encapsulation efficiency and drug loading of ADNPs were calculated using the following equations:

$$EE\ (\%) = \frac{\text{Weight of encapsulated Ac2} - 26 \text{ in ADNPs}}{\text{Weight of total Ac2} - 26} \times 100\%$$

$$DL\ (\%) = \frac{\text{Weight of encapsulated Ac2} - 26 \text{ in ADNPs}}{\text{Total weight of ADNPs formulation}} \times 100\%$$

2.5. Stability study

The size and PDI of ADNPs at 37 °C were monitored over time. Meanwhile, the stability of ADNPs in plasma was investigated by incubating them with human serum albumin (HSA) solution at 37 °C. Briefly, 100 µl HSA solution (4%, w/v) was incubated with ADNPs at the concentration varying from 0.3 mg/ml to 3 mg/ml. After being incubated for predetermined time intervals, the absorbance of different samples at 600 nm defined as turbidity was measured by a microplate reader (Thermo Scientific, USA) [30].

2.6. Cell cytotoxicity of LDNPs

To evaluate the biocompatibility of LDNPs, Raw264.7 and HUVEC cells were seeded in 96-well plates at a density of 1×10^4 per well in culture medium. LDNPs at the concentration ranging from 0 to 250 µg/ml were added to different cell samples and incubated with cells for 24 h. Then the cell viability was detected by MTT assay. Briefly, the culture medium was discarded and 20 µl MTT (5 mg/ml) was added to each well. After 4 h incubation, the culture medium was removed and 150 µl DMSO was added to dissolve the formazan crystals. All samples were incubated for another 15 min at 37 °C. Finally, the absorbance at 490 nm was determined by a microplate reader. The relative cell viability was calculated using the following formula:

$$\text{Cell viability (\%)} = \frac{A_{\text{sample}} - A_{\text{blank}}}{A_{\text{negative control}} - A_{\text{blank}}} \times 100\%$$

2.7. In vitro release of Ac2–26 from ADNPs

The in vitro release behavior of Ac2–26 from ADNPs was measured by a dialysis method reported previously [31]. Briefly, 1 ml ADNPs and free Ac2–26 solution (500 µg/ml of Ac2–26, dissolved in phosphate buffer containing 10% propylene glycol) were placed into a dialysis bag with the molecular weight cut-off of 10 kD, respectively. Then, the dialysis bag was immersed in the glass bottle with 10 ml release medium (phosphate buffer containing 10% propylene glycol) in a shaker at 37 °C/70 rpm. At the indicated incubation time, 200 µl of release medium was collected and substituted by equal volume of fresh release medium. The concentration of cumulative release of Ac2–26 was determined by HPLC.

2.8. Synthesis of Cy5-Ac2–26 peptides

Cy5-Ac2–26 peptides were synthesized via an amide reaction between the succinimide ester grafted on Cy5-NHS and the carboxyl residuals of Ac2–26. Briefly, Cy5-NHS (1 mg) and Ac2–26 (12 mg) were dissolved in DMSO at a molar ratio of 1:3. Triethylamine (TEA, 50 µl) was subsequently added in a dropwise way into the mixture under stirring at room temperature. After stirring at dark atmosphere for 24 h, the reaction solution was transferred to a dialysis bag and dialyzed against deionized water for 1 d at room temperature. The obtained solution was frozen and lyophilized to form Cy5-Ac2–26 peptides. The structure of Cy5-Ac2–26 peptides was confirmed by ^{1}H NMR (400 MHz, Bruker AMX-400, USA).

2.9. Pharmacokinetic studies

Healthy male Sprague–Dawley (SD) rats were randomly divided into two groups ($n = 6$). And each rat was intravenously injected with Cy5-Ac2–26 solution or Cy5-Ac2–26 loaded PEGylated lipid nanoparticles (Cy5-ADNPs) at the peptide dose of 0.5 mg/kg. Blood samples (0.5 ml) were obtained from retro-orbital plexus at 5 min, 15 min, 0.5, 1, 2, 4, 8, 12, 24 and 48 h after injection and then centrifuged at 5000 rpm for 10 min to collect plasma samples. The upper plasma samples were diluted by adding 1 ml deionized water. The fluorescence intensity of Cy5-Ac2–26 peptides was determined by a fluorescence spectrophotometer (SHIMADZU, Japan). The pharmacokinetic parameters of AUC_{0-t} and $T_{1/2}$ were analyzed by DAS software.

2.10. Establishment of adjuvant-induced arthritis (AIA) rat model

The arthritis model was induced using a complete freund adjuvant (CFA, containing 10 mg/ml of mycobacterium tuberculosis) [32,33]. Briefly, 50 µl CFA was subcutaneously injected into the paws of SD rats at Day 1. The swelling of the rat limbs was monitored every day. All animals were housed in standard condition that met the requirements of the animal ethics committee.

2.11. In vivo biodistribution of ADNPs

For biodistribution assay, the AIA rats were randomly divided into two groups ($n = 3$). The AIA rats received intravenous injection of Cy5-Ac2–26 solution or Cy5-ADNPs (at the peptide dose of 0.5 mg/kg), respectively. The distribution of fluorescence signals in rats was evaluated by an *in vivo* imaging system (IVIS, Perkin Elmer, USA) after 2, 6 and 24 h intravenous injection, respectively. Subsequently, rats were euthanized. The heart, liver, spleen, lung, kidney, and joint tissues were collected. The fluorescence intensity of these organs in each group was measured after the background subtraction using the IVIS system. The biodistribution behavior of ADNPs was further visualized through an *in vivo* imaging system.

2.12. In vivo therapeutic efficacy

To further investigate the therapeutic efficacy of ADNPs, arthritic rats were randomly divided into 3 groups ($n = 7$). Healthy rats were severed as a normal control. The AIA rats were intravenously injected with the equal volume of PBS, free Ac2–26, and ADNPs (at the peptide dose of 0.75 mg/kg) every day for one week, respectively. During the period of the treatments, the body weight, paw thickness and joint score of the AIA rats were monitored every day in each group. The joint score determined by grading from score of 0 (no observable erythema or swelling) to 4 (severe swelling and erythema) was given for each paw. The swelling and ulceration degree of 4 paws were scored, finally resulting in a maximum possible score of 16 for each animal [34]. After 14 d, the rats were sacrificed to collect joint tissues. The joint tissues from each group were cut up and homogenized. The concentration of

inflammatory cytokines (TNF-α, IL-1β, IL-6, IL-17A) in joint homogenates was measured by ELISA. The joint ankles from each group were soaked in 4% paraformaldehyde solution for 3 d and then incubated in 15% EDTA-2Na decalcification solution until the samples could be easily sliced. The joint slices were finally stained with hematoxylin and eosin to observe the inflammatory cell infiltration and cartilage erosion. For the immunohistochemical analysis, slices were incubated with specific antibodies directed against IL-17A and myeloperoxidase (MPO), followed by the incubation with appropriate secondary antibodies.

2.13. Flow cytometry analysis of Th17 and T_{reg}

After the treatment was terminated on Day 24, the popliteal draining lymph nodes were harvested and passed through a 300-mesh cell sieve to form single-cell suspensions. The Th17 cell (CD4+IL-17+) and T_{reg} cell (CD4+Foxp3+) subsets in draining lymph nodes were analyzed using flow cytometry.

2.14. Statistical analysis

All the experiment data were expressed by mean ± standard deviation (SD). Statistical analysis of the data and the calculation of AUC score were calculated using GraphPad Prism 7.0 software. Significant differences between two comparative groups were analyzed by student's *t*-test. The one-way analysis of variance (ANOVA) was used to evaluate the significance of multiple groups. And $P < 0.05$ was considered as a significant difference.

3. Results and discussion

3.1. Preparation and characterization of LDNPs and ADNPs

Fig. 1A-1B showed the size distribution of PEGylated lipid nanoparticles with/without Ac2–26 peptide loadings (ADNPs/LDNPs). The average diameter was 101.23 nm ± 0.41 nm for LDNPs and 123.59 nm ± 6.66 nm for ADNPs, respectively. This result revealed that the loading of Ac2–26 peptides slightly increased the diameter of nanoparticles. The TEM images of LDNPs and ADNPs were shown in Fig. 1C and 1D, respectively. Fig. 1E showed the absorption spectra of LDNPs and ADNPs, together with free Ac2–26 peptides. The free Ac2–26 peptides showed a characteristic absorption band at ~ 220 nm. While LDNPs showed an absorption band at ~ 247 nm. The two absorption bands were observed in the spectrum of ADNPs. The EE and DL of ADNPs for Ac2–26 peptides was calculated to be approximately 92.8% and 3.4%, respectively.

3.2. Stability study

The average size and PDI of ADNPs maintained nearly unchanged at 37 °C within 72 h (Fig. 1F), suggesting that they had good stability on standing. To estimate the plasma stability of ADNPs, the ADNPs with different concentrations were incubated with HSA solution over time. There was no
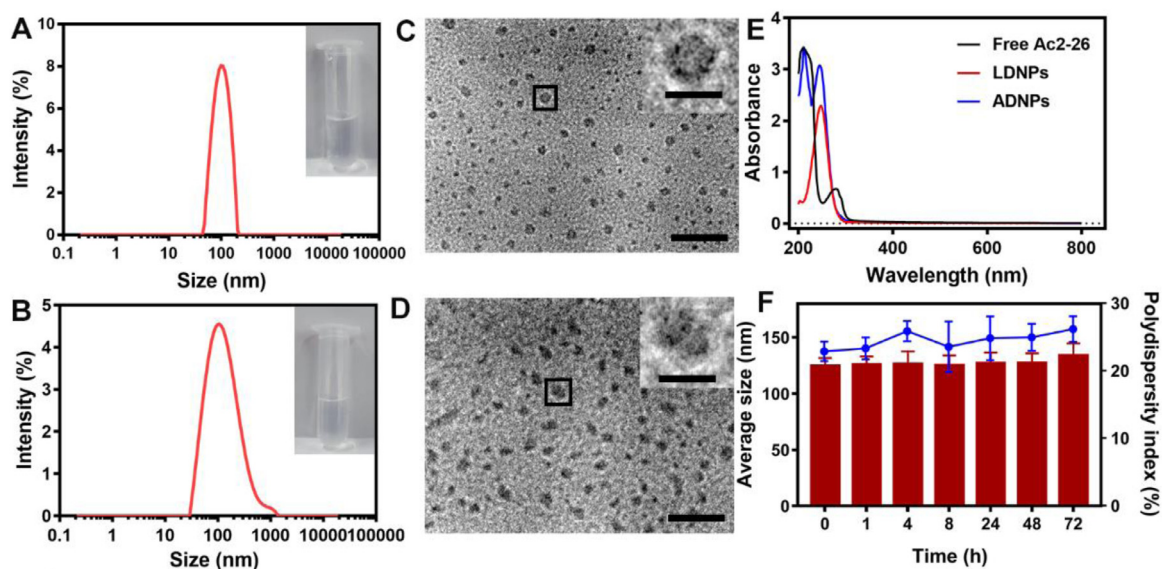
Fig. 1 – Characterization of nanoparticles. The size of LDNPs (A) and ADNPs (B). Representative TEM images of LDNPs (C) and ADNPs (D). Scale bar is 100 nm. The magnification of single nanoparticle is fivefold of representative images. Scale bar is 20 nm. (E) Representative UV–vis spectra of free Ac2–26, LDNPs and ADNPs. (F) Stability of ADNPs at 37 °C.
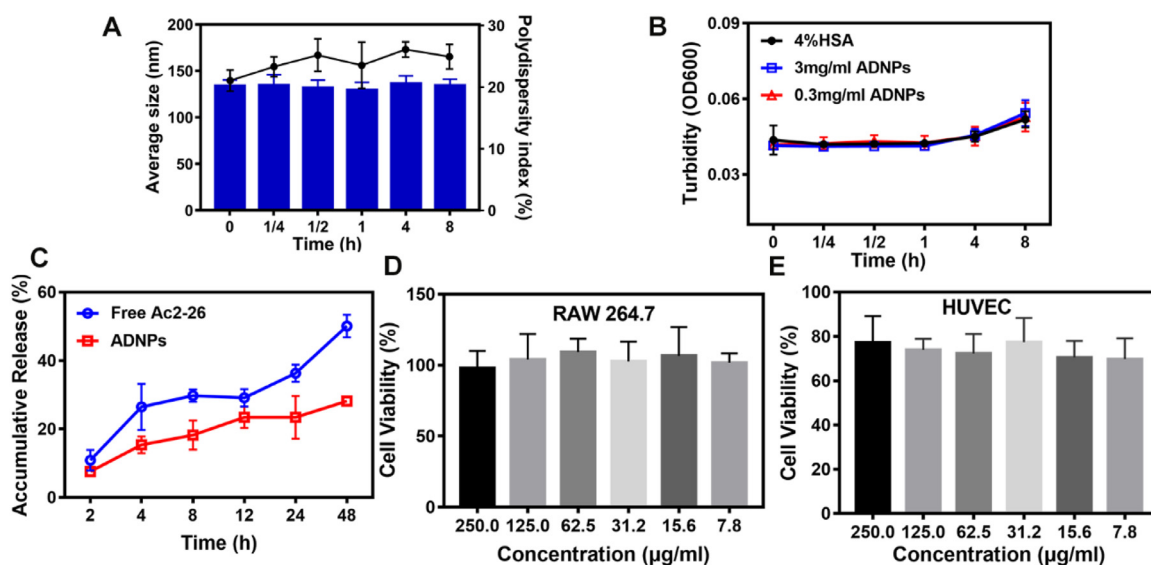

Fig. 2 – (A) Stability of ANDPs in HSA solution at 37 °C. (B) Turbidity of ADNPs in HSA solution. (C) *In vitro* **release behavior of Ac2–26 peptides. Viability of Raw 264.7 (D) and HUVEC (E) cells after 24 h incubation with LDNPs at different concentrations. Results were shown as mean ± SD ($n = 5$).**

significant change observed in average size and the turbidity of the solutions (Fig. 2A-2B), suggesting that ADNPs remained stable in plasma without aggregations.

3.3. Cytotoxicity study of LDNPs

To determine the biocompatibility of LDNPs, RAW264.7 and HUVEC cells were selected. As can be seen in Fig. 2D-2E, there was no significant cytotoxicity for both RAW264.7 and HUVEC cells observed at the concentration of PEGylated lipid nanoparticles from 7.8 to 250.0 µg/ml, suggesting that they had good cytocompatibility.

3.4. In vitro release of Ac2–26 from ADNPs

To simulate the release of Ac2–26 from ADNPs at physiological conditions, phosphate buffer was used as a release medium. Propylene glycol at the final concentration of 10% (v/v) was added to increase the solubility of Ac2–26 peptides in the release medium. As shown in Fig. S1, the propylene glycol would not degrade the nanoparticles. The cumulative release curve of Ac2–26 peptides was shown in Fig. 2C. Within the first 4 h, 30% of Ac2–26 peptides was released from the free Ac2–26 group, while only ~15% of Ac2–26 peptides was released from ADNPs. After 48 h, the cumulative release of Ac2–26 peptides
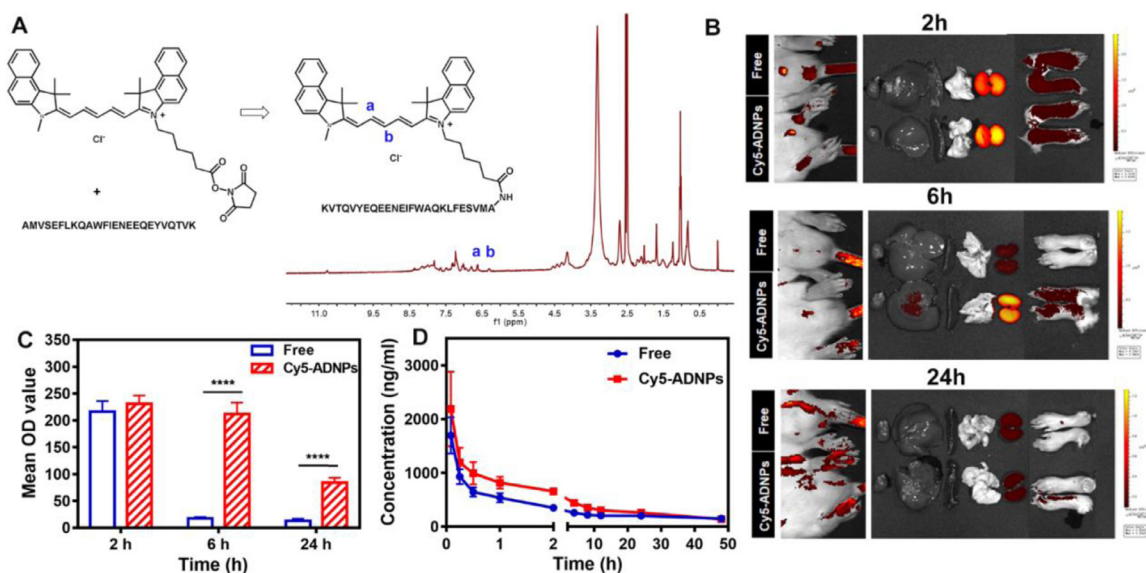
Fig. 3 – (A) The synthesis scheme and ^{1}H NMR (DMSO–d6) spectra of Cy5-Ac2–26. (B) Representative biodistribution images of arthritic rats after the intravenous injection of free Cy5-Ac2–26 peptides (Free) and Cy5-ADNPs at different time points. (C) Fluorescent signal comparison in paws segregated of arthritic rats after the intravenous injection of free Cy5-Ac2–26 peptides and Cy5-ADNPs at 2, 6 and 24 h, respectively. These results were calculated by Image J software. Results were shown as mean ± SD ($n = 3$). (D) Pharmacokinetics profiles after the intravenously injection of free Cy5-Ac2–26 peptides and Cy5-ADNPs at the dose of 0.5 mg/kg. Results were shown as mean ± SD ($n = 6$).

from the free Ac2–26 group increased to ∼55%. While, less than 30% of Ac2–26 peptides was released from ADNPs. These results indicated that Ac2–26 peptides maintained a slow and sustained release from ADNPs.

3.5. Biodistribution of ADNPs in AIA rats

To estimate the targeting ability of ADNPs to inflamed joint, the Cy5-Ac2–26 peptides were synthesized as previously mentioned. The ^{1}H NMR spectra of Cy5-Ac2–26 peptides was shown in Fig. 3A (400 MHz). Compared with the ^{1}H NMR spectra of Cy5-NHS and Ac2–26 peptides shown in Fig.S2-S3, the peaks of alkenyl appeared at 6.25 ppm and 6.58 ppm, indicating the successful linking of Cy5-NHS and Ac2–26 peptides. After the AIA model was established, the biodistribution of ADNPs in AIA rats was observed by an *in vivo* imaging system. The Cy5-ADNPs were prepared via thin film hydration method as ADNPs. As shown in Fig. 3B-C, the fluorescence signals of Cy5 were observed in the inflamed joints in both the Cy5-Ac2–26 (Free) and the Cy5-ADNPs treated groups after 2 h injection. The accumulation of nanoparticles in the arthritic sites was still obvious after 6 h injection. While almost no fluorescence signals appeared in the hind paws of the free Cy5-Ac2–26 treated group. The strong fluorescence signal of the Cy5-ADNPs group retained at the paws of AIA rat even after 24 h injection, indicating the ADNPs possessed excellent inflammation-homing and retention capacity in AIA rats.

3.6. Pharmacokinetics study

In this experiment, the fluorescence intensity of Cy5-Ac2–26 peptides in plasma was determined to analyze the

Table 1 – Pharmacokinetic parameters.

	Free	Cy5-ADNPs
AUC_{0-t} (μg/l·h)	9892.55 ± 59.31	14,187.27 ± 88.02
$T_{1/2}$ (h)	17.11 ± 1.58	36.81 ± 3.36

pharmacokinetic behavior of ADNPs. As shown in Fig. 3D, the concentration of Cy5-Ac2–26 peptides in the Cy5-ADNPs treated group declined slower than that in the free Cy5-Ac2–26 treated group. After 48 h injection, there were still 145 ng/ml Cy5-Ac2–26 peptides in plasma from the Cy5-ADNPs treated group. The pharmacokinetic parameters were shown in Table 1. The 1.48-fold increase in AUC_{0-t} was observed in the Cy5-ADNPs group, compared with the free Cy5-Ac2–26 group. The $T_{1/2}$ of Cy5-ADNPs group was 2-fold higher than that in the free Cy5-Ac2–26 group. These results demonstrated that Cy5-ADNPs greatly contributed to the prolonged blood circulation and *in vivo* $T_{1/2}$ of Cy5-Ac2–26 peptides.

3.7. Therapeutic efficacy of ADNPs in AIA rats

The treatment procedure was briefly showed in Fig. 4A. The CFA was subcutaneously injected into the paws of rats on Day 1 to induce the development of arthritis. The arthritis model was almost established on Day 10. The arthritic rats were then randomly divided into 3 groups and treated with different formulations. As shown in Fig. 4B, the hind paws in the PBS treated group showed severe swelling, edema and even ulceration. The free Ac2–26 treatment slightly decreased the swelling degree of joints. After the treatment
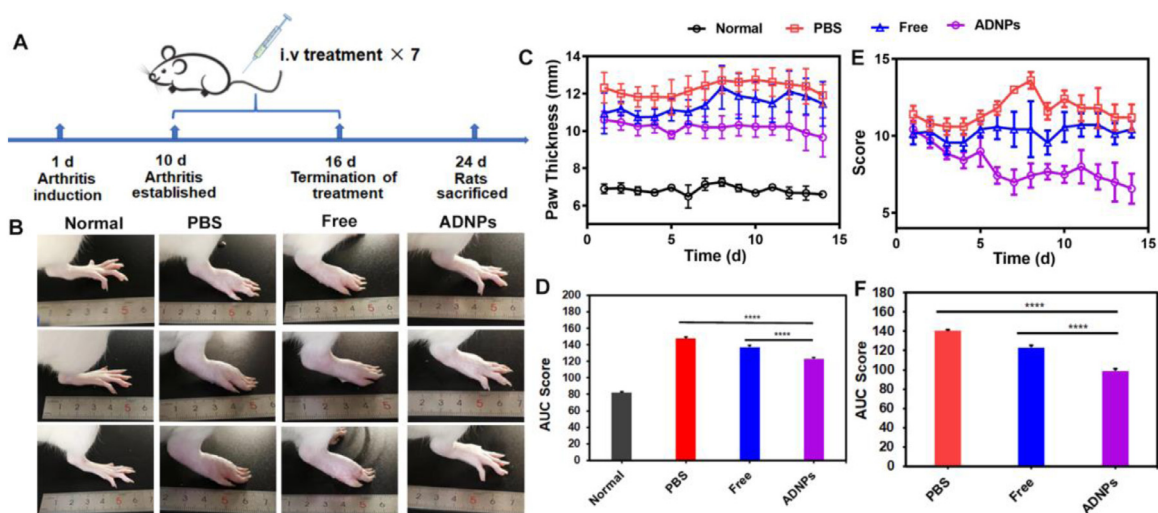
Fig. 4 – *In vivo* therapeutic efficacy of ADNPs in AIA rats. (A) Overall experimental schedule for the treatment of arthritic rats. (B) Representative images of the hind paws after the treatment with PBS, free Ac2–26 peptides and ADNPs for 14 d, respectively. The paw thickness (C) and AUC score (D) after the treatment of PBS, free Ac2–26 peptides and ADNPs. The swelling degree score (E) and AUC score (F) after the treatment of PBS, free Ac2–26 peptides and ADNPs. Results were shown as mean ± SD ($n = 7$). *$P < 0.05$, **$P < 0.01$, ***$P < 0.001$, ****$P < 0.0001$.

of ADNPs, no obvious swelling of joint was observed. The paw thickness after these treatments was shown in Fig. 4C. Compared with the PBS group, the limited reduction of the paw thickness was observed in the free Ac2–26 group. In contrast, the development of RA was fully suppressed in the ADNPs treated group. Fig. 4E showed the change of joint score after the treatment of PBS, free Ac2–26 and ADNPs. In comparison with the PBS treatment, the free Ac2–26 treatment slightly inhibited the development of joint swelling. While the rats receiving the ADNPs treatment showed the dramatical decrease in joint score. The calculation of the area under these curves (AUC score) provided a direct comparison between these groups (Fig. 4D and 4F). Compared with the PBS group and the free Ac2–26 group, the ADNPs group showed the lowest AUC score value in both the paw thickness and joint score. All these results indicated that ADNPs were highly effective in inflammatory resolution.

To further confirm the pathological condition of inflamed joints after the treatment of PBS, free Ac2–26 peptides and ADNPs, the ankle joints of rats were analyzed by hematoxylin-eosin staining. As shown in Fig. 5A, the aggressive hyperplasia of synovium narrowed the articular cavity. However, after the treatment of ADNPs, the articular cavity recovered with very few inflammation infiltration and cartilage erosion. The score of pathological staining was also evaluated. The extensive inflammation infiltration, tissue damage and cartilage destruction were observed after the treatment of PBS and free Ac2–26 (Fig. 5B-5C). However, there was a significantly decreased score in the inflammation infiltration and cartilage erosion after the treatment of ADNPs, indicating that ADNPs treatment had the favorable effect on the tissue repair in inflammatory remission.

3.8. Inflammation resolution mediated by ADNPs

MPO, the most abundant granule enzyme produced by neutrophils, is rapidly released upon neutrophil activation in inflammatory process. MPO could amplify inflammatory response in a neutrophil-dependent behavior and finally delay the inflammatory resolution [35]. Therefore, the level of MPO may be an indicator of neutrophil infiltration, which is highly correlated with the inflammation resolution. In Fig. 5A, the expression of MPO (black arrow) was highest in the PBS treatment group, suggesting the massive inflammation infiltration in joint tissues. The free Ac2–26 treatment could slightly attenuate the expression of MPO. While the level of MPO after the treatment of ADNPs was significantly declined, indicating that they had the excellent ability in inflammation resolution.

IL-17A produced by Th17 cells is a key player in the pathogenesis of autoimmune diseases. IL-17A could not only initiate the activation of autoreactive T cells [36], but also enhance the release of invasive matrix metalloproteinases (MMPs) in synovitis, mediating the destruction of joint tissues [37]. As shown in Fig. 5A, the expression of IL-17A (black arrow) was clearly visible after the treatment of PBS and free Ac2–26, indicating an overactive immune response. While the level of IL-17A after the treatment of ADNPs was reduced to the similar level of the normal group, suggesting a balanced immune state.

The rats in each treatment group were euthanasia after 14 d observation. The homogenates of joint tissue were collected for evaluating the level of inflammatory cytokines. As shown in Fig. 5D-5G, the treatment of ADNPs significantly inhibited the expression of TNF-α, IL-1β, IL-6 and IL-17A. While the free Ac2–26 treatment was unable to effectively decrease the inflammatory level. It was reported that the
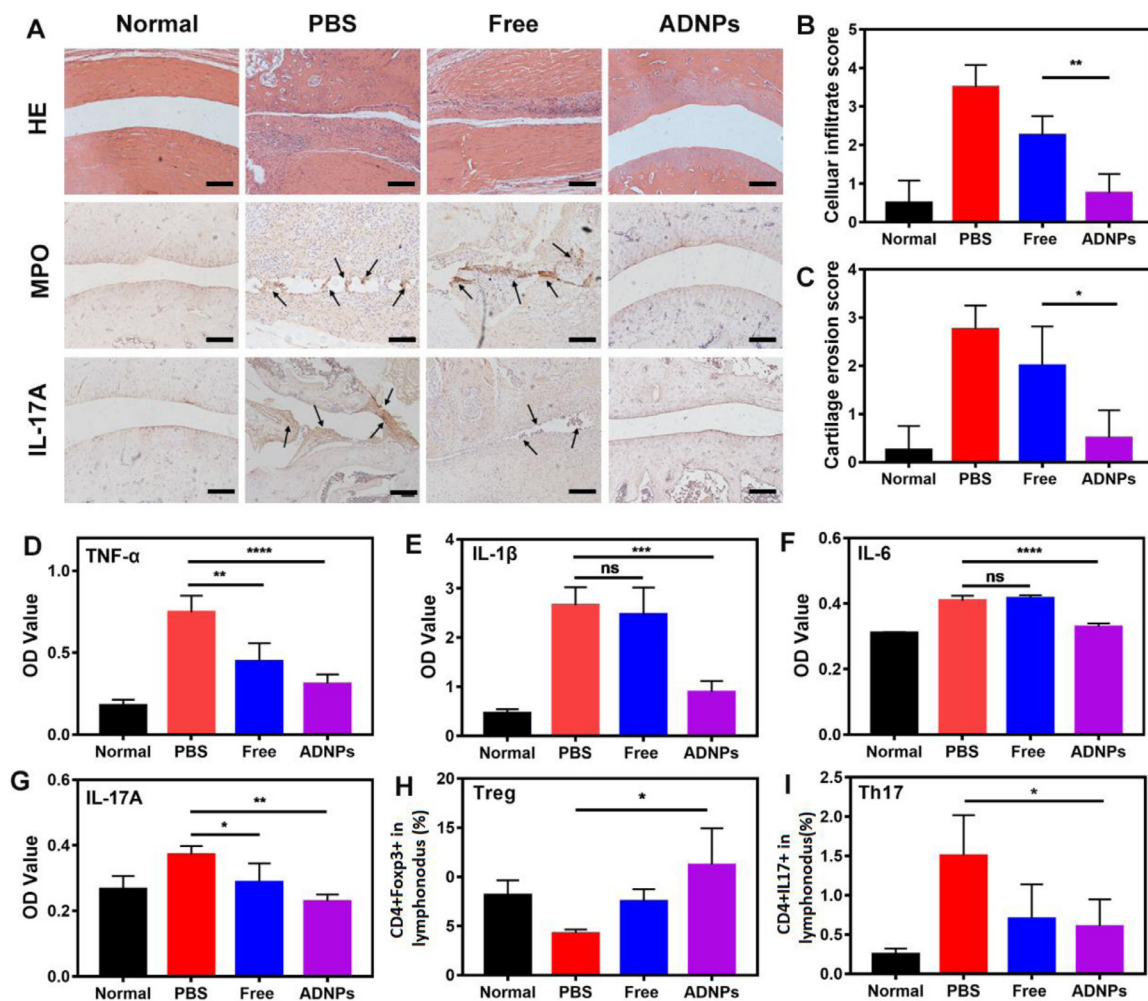
Fig. 5 – (A) Representative histological images of HE staining, MPO and IL-17A immunohistochemical staining for different treatment groups. Scale bar is 200 μm. The average score of cell infiltration (B) and cartilage erosion (C) analyzed by the results of HE staining. The inflammatory levels of TNF-α (D), IL-1β (E), IL-6 (F) and IL-17A (G) in joint tissues after the treatment with PBS, free Ac2–26 peptides and ADNPs. Normal rats served as the control group. The flow cytometric analysis of T$_{reg}$ (H) and Th17 (I) in draining lymph nodes. Results were shown as mean ± SD ($n = 7$). *$P < 0.05$, **$P < 0.01$, ***$P < 0.001$, ****$P < 0.0001$.

imbalance between Th17 cells and T$_{reg}$ cells was essential to the pathogenesis of RA [38]. The equilibrium of Th17 and T$_{reg}$ cells would promote the restoration of immune homeostasis in RA [39]. The proportion of T$_{reg}$ cells and Th17 cells in draining lymph nodes was showed in Fig. 5H and 5I, respectively. The free Ac2–26 treatment was unable to increase the proportion of T$_{reg}$. On the contrary, the significant increase of the population of T$_{reg}$ and decrease of Th17 cells were observed after the treatment of ADNPs. In general, these results revealed that the treatment of ADNPs in AIA rats could effectively achieve inflammation resolution by reducing inflammatory levels, improving joint pathology and restoring immune homeostasis.

3.9. Biocompatibility study

Considering the frequent systemic adverse effect in current treatments, we further studied the safety of ADNPs. As shown in Fig. 6A, the count of red blood cells (RBC) for all the treatments was nearly the same as the normal group. Interestingly, the count of white blood cells (WBC) and platelets (PLT) after the treatment of PBS significantly increased compared with normal group (Fig. 6B-6C). This might be due to the elevated inflammatory response after the treatment of PBS. However, there was no significant difference in the count of WBC and PLT after the treatment of free Ac2–26 and ADNPs, compared to the normal group. The body weight of rats in each treatment group was showed in Fig. 6D. There was no obvious weight loss during these treatments. These results indicated that the therapeutic strategy based on ADNPs possesses an acceptable biocompatibility and hemocompatibility.

3.10. Discussion

RA is highly chronic and requires life-long managements. Long-term therapy using current anti-inflammatory strategies is usually lack of adequate responsiveness and accompanied
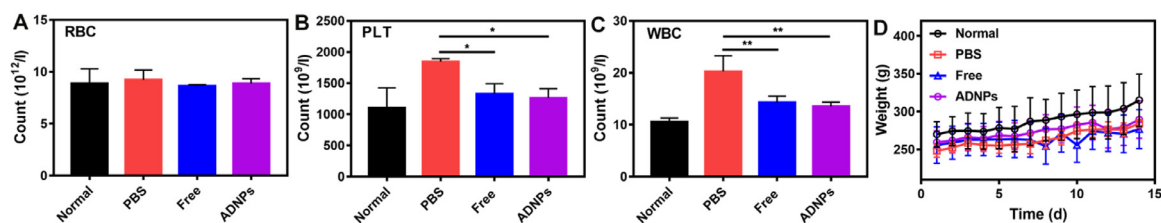
Fig. 6 – Biocompatibility studies of ADNPs in AIA rats. (A) RBC, (B) platelet and (C) WBC counts in blood after the treatment of PBS, free Ac2–26 peptides and ADNPs. Normal rats served as the control group. (D) The body weight of arthritis rats in each treatment group. Results were shown as mean ± SD, $n = 7$. *$P < 0.05$, **$P < 0.01$.

with serious side effects. Recent studies on the pathogenesis of inflammation showed that the persistence of chronic inflammation might be not only caused by the complicated and enormous inflammatory networks, but also the absence of resolution mechanism [40]. This resolution function is often fulfilled by some specific mediators *in vivo* such as resolving E1, lipoxin and annexin A1 [41]. They can facilitate the inflammation resolution, restore inflamed tissue and maintain the immune homeostasis. For example, the lipid pro-resolving mediator, resolving E1, could inhibit the development of inflammatory diseases by blocking the neutrophil recruitment [42]. Annexin A1, a protein with a molecular weight of 37 kD, was able to activate anti-inflammatory signaling by binding to the G-protein-coupled receptors [43]. Therefore, therapeutic strategies based on the pro-resolving therapy might offer a promising option for the treatment of inflammatory diseases including RA.

Ac2–26, an annexin A1 mimic peptide, has the similar efficacy of inflammation resolution as annexin A1. But it has better stability and lower immunogenicity than Annexin A1. However, the direct administration of Ac2–26 peptides may result in low bioavailability due to the rapid degradation of peptides *in vivo*. To improve the bioavailability of Ac2–26 *in vivo*, we constructed LDNPs by the co-assembly of L-AP and DSPE-PEG2k to encapsulate and deliver Ac2–26 to inflamed joints. When the Ac2–26 peptide was released from ADNPs in inflamed joints, it could bind to the FPR2/ALX receptors on cell surface, ultimately playing an important role in the resolution pathway of inflammation. The obtained nanoparticles displayed a uniformed diameter around 123.59 nm and negative charge of −9.4 mV, which is suitable for intravenous administration. The ADNPs showed a desirable stability when kept at 37 °C or incubated with serum components *in vitro*, laying a good foundation for *in vivo* application. Using a thin-film method, Ac2–26 peptides could be incorporated into the hydrophobic core of ADNPs at a relatively high encapsulation efficiency. And *in vitro* drug release demonstrated that ADNPs could slowly release Ac2–26 peptides in PBS. When incubated with macrophages and vascular endothelial cells, the ADNPs did not affect the cell viability, displaying a favorable cytocompatibility. After being administrated *in vivo*, the ADNPs showed prolonged circulation time and improved the accumulation of Ac2–26 peptides in inflamed joints due to the passive targeted delivery of nanosized ADNPs. After one-week treatment, the ADNPs significantly inhibited the joint inflammation and ameliorated the pathology of arthritic joint.

During the development of RA, massive neutrophils would traffic to arthritic sites and then be activated by inflammatory signals. The activated neutrophils would consequently produce destructive granule enzymes such as MPO, leading to the persistent inflammation and tissue damage [44]. In Fig. 6A (middle pane), we found that the treatment of ADNPs significantly suppressed the level of MPO, indicating that the treatment was able to reduce neutrophil influx in inflamed sites.

IL-17A, mainly generated by Th17, is known as the key player in the pathogenesis of RA, driving the excessive autoimmune response [45]. On the contrary, the T_{reg} is essential in maintaining the immune tolerance in autoimmune diseases by restraining the overshooting of immune activation [46]. Therefore, permanent immune homeostasis usually depends on the balance between Th17 and T_{reg} [47]. The occurrence of RA disrupts the equilibrium between these cell subsets by increasing the level of Th17 and decreasing the level of T_{reg}. As a result, regulating the level of Th17 and T_{reg} to the normal range would hold promise to reverse the development of RA. We found that the treatment of ADNPs obviously reduced the level of IL-17A produced by Th17 cells and up-regulated the level of T_{reg} in draining lymph node to the normal level (Fig. 6G). Furthermore, the treatment of ADNPs showed more effective therapeutic index than the treatment of free Ac2–26 peptides.

Collectively, the treatment of ADNPs could exert a favorable inflammation resolution by inhibiting the neutrophils influx to inflamed sites, facilitating the tissues repair and promoting the balance of immune response. To the best of our knowledge, there has no drug designed for aiming at the pro-resolving pathways in the clinical applications. Thus, ADNPs formulation would provide new therapeutic option for RA therapy.

4.   Conclusion

We synthesized LDNPs by the co-assembly of L-AP and DSPE-PEG2k to deliver hydrophobic Ac2–26 peptides for the treatment of RA. The ADNPs showed prolonged circulation time *in vivo* and enhanced accumulated in inflamed joints. In arthritic rat model, the treatment of ADNPs was able to reduce the swelling degree of paw thickness, inhibit the inflammatory level in inflamed joints and promote the

immune homeostasis. Our results highlight the potential of the ADNPs as a candidate for RA treatment.

Conflicts of interest

No competing interest exists.

Acknowledgments

Supplementary materials

Supplementary material associated with this article can be found, in the online version, at doi:10.1016/j.ajps.2021.03.001.

REFERENCES

[1] Myasoedova E, Davis J, Matteson EL, Crowson CS. Is the epidemiology of rheumatoid arthritis changing? Results from a population-based incidence study, 1985-2014. Ann Rheum Dis 2020;79(4):440–4.

[2] McInnes IB, Schett G. Pathogenetic insights from the treatment of rheumatoid arthritis. Lancet 2017;389(10086):2328–37.

[3] Angelotti F, Parma A, Cafaro G, Capecchi R, Alunno A, Puxeddu I. One year in review 2017: pathogenesis of rheumatoid arthritis. Clin Exp Rheumatol 2017;35(3):368–78.

[4] O'Neil LJ, Kaplan M. Neutrophils in rheumatoid arthritis: breaking immune tolerance and fueling disease. Trends Mol Med 2019;25(3):215–27.

[5] Wang Q, Sun X. Recent advances in nanomedicines for the treatment of rheumatoid arthritis. Biomater Sci 2017;5(8):1407–20.

[6] Yang MD, Feng XR, Ding JX, Chang F, Chen XS. Nanotherapeutics relieve rheumatoid arthritis. J Control Release 2017;252(2):108–24.

[7] Perretti M, Cooper D, Dalli J, Norling LV. Immune resolution mechanisms in inflammatory arthritis. Nat Rev Rheumatol 2017;13(2):87–99.

[8] Kłodziński Ł, Wisłowska M. Comorbidities in rheumatic arthritis. Reumatologia 2018;56(4):228–33.

[9] Fullerton JN, Gilroy DW. Resolution of inflammation: a new therapeutic frontier. Nat Rev Drug Discov 2016;15(8):551–67.

[10] Schett G, Neurath MF. Resolution of chronic inflammatory disease: universal and tissue-specific concepts. Nat Commun 2018;9(1):3261.

[11] Gilroy DW, Lawrence T, Perretti M, Rossi AG. Inflammatory resolution: new opportunities for drug discovery. Nat Rev Drug Discov 2004;3(5):401–16.

[12] Barden AE, Moghaddami M, Mas E, Phillips M, Cleland LG, Mori TA. Specialised pro-resolving mediators of inflammation in inflammatory arthritis. Prostag Leukotr Ess 2016;107(3):24–9.

[13] Ortega-Gómez A, Perretti M, Soehnlein O. Resolution of inflammation: an integrated view. EMBO Mol Med 2013;5(5):661–74.

[14] Perretti M, Leroy X, Bland EJ, Montero-Melendez T. Resolution pharmacology: opportunities for therapeutic innovation in inflammation. Trends Pharmacol Sci 2015;36(11):737–55.

[15] Bena S, Brancaleone V, Wang JM, Perretti M, Flower RJ. Annexin A1 interaction with the FPR2/ALX receptor: identification of distinct domains and downstream associated signaling. J Biol Chem 2012;287(29):24690–7.

[16] Basil MC, Levy BD. Specialized pro-resolving mediators: endogenous regulators of infection and inflammation. Nat Rev Immunol 2016;16(1):51–67.

[17] Yu C, Chen H, Qi X, Chen P, Di G. Annexin A1 mimetic peptide Ac2-26 attenuates mechanical injury induced corneal scarring and inflammation. Biochem Biophys Res Commun 2019;519(2):396–401.

[18] Maderna P, Yona S, Perretti M, Godson C. Modulation of phagocytosis of apoptotic neutrophils by supernatant from dexamethasone-treated macrophages and annexin-derived peptide Ac(2-26). J Immunol 2005;174(6):3727–33.

[19] Kamaly N, Fredman G, Subramanian M, Gadde S, Pesic A, Cheung L, Fayad ZA, et al. Development and *in vivo* efficacy of targeted polymeric inflammation-resolving nanoparticles. Proc Natl Acad Sci USA 2013;110(16):6506–11.

[20] Fredman G, Kamaly N, Spolitu S, Milton J, Ghorpade D, Chiasson R, Kuriakose G, et al. Targeted nanoparticles containing the proresolving peptide Ac2-26 protect against advanced atherosclerosis in hypercholesterolemic mice. Sci Transl Med 2015;7(275):ra220.

[21] Syed A, Devi VK. Potential of targeted drug delivery systems in treatment of rheumatoid arthritis. J Drug Deliv Sci Tec 2019;53(1):1–10.

[22] Pirmardvand Chegini S, Varshosaz J, Taymouri S. Recent approaches for targeted drug delivery in rheumatoid arthritis diagnosis and treatment. Artif Cells Nanomed Biotechnol 2018;46(sup2):502–14.

[23] Chen M, Daddy JCK, Xiao Y, Ping Q, Zong L. Advanced nanomedicine for rheumatoid arthritis treatment: focus on active targeting. Expert Opin Drug Deliv 2017;14(10):1141–4.

[24] Vijayakumar MR, Kosuru R, Vuddanda PR, Singh SK, Singh S. Trans resveratrol loaded DSPE PEG 2000 coated liposomes: an evidence for prolonged systemic circulation and passive brain targeting. J Drug Deliv Sci Tec 2016;33(3):125–35.

[25] Kim DH, Im BN, Hwang HS, Na K. Gemcitabine-loaded DSPE-PEG-PheoA liposome as a photomediated immune modulator for cholangiocarcinoma treatment. Biomaterials 2018;183(11):139–50.

[26] Wang Q, He LM, Fan DH, Liang WL, Fang JY. Improving the anti-inflammatory efficacy of dexamethasone in the treatment of rheumatoid arthritis with polymerized stealth liposomes as a delivery vehicle. J Mater Chem B 2020;8(9):1841–51.

[27] Gosenca M, Obreza A, Pečar S, Gašperlin M. A new approach for increasing ascorbyl palmitate stability by addition of non-irritant co-antioxidant. AAPS Pharm Sci Tech 2010;11(3):1485–92.

[28] Cheng S, Grest GS. Dispersing nanoparticles in a polymer film via solvent evaporation. ACS Macro Lett 2016;5(6):694–8.

[29] Zhang Y, Ng W, Feng X, Cao F, Xu H. Lipid vesicular nanocarrier: quick encapsulation efficiency determination and transcutaneous application. Int J Pharm 2017;516(1–2):225–30.

[30] Han J, Wang Q, Zhang Z, Gong T, Sun X. Cationic bovine serum albumin based self-assembled nanoparticles as siRNA delivery vector for treating lung metastatic cancer. Small 2014;10(3):524–35.

[31] Solomon D, Gupta N, Mulla NS, Shukla S, Guerrero YA, Gupta V. Role of *in vitro* release methods in liposomal formulation development: challenges and regulatory perspective. AAPS J 2017;19(6):1669–81.

[32] He L, Fan D, Liang W, Wang Q, Fang J. Matrix metalloproteinase-responsive PEGylated lipid nanoparticles

for controlled drug delivery in the treatment of rheumatoid arthritis. ACS Appl Bio Mater 2020;3(5):3276–84.

[33] Wang Q, Jiang J, Chen W, Jiang H, Zhang Z, Sun X. Targeted delivery of low-dose dexamethasone using PCL-PEG micelles for effective treatment of rheumatoid arthritis. J Control Release 2016;230(3):64–72.

[34] Leech M, Metz C, Bucala R, Morand EF. Regulation of macrophage migration inhibitory factor by endogenous glucocorticoids in rat adjuvant-induced arthritis. Arthritis Rheum 2000;43(4):827–33.

[35] Odobasic D, Yang Y, Muljadi RCM, O'Sullivan KM, Kao WP, Smith M, Morand EF, et al. Endogenous myeloperoxidase is a mediator of joint inflammation and damage in experimental arthritis. Arthritis Rheumatol 2014;66(4):907–17.

[36] Chen WQ, Wang Q, Ke YN, Lin J. Neutrophil function in an inflammatory milieu of rheumatoid arthritis. J Immunol Res 2018;2018(12):1–12.

[37] Malemud CJ. Matrix metalloproteinases and synovial joint pathology. Prog Mol Biol Transl Sci 2017 2017;148:305–25.

[38] Wang T, Li S, Yang Y, Zhang K, Dong S, Wang X, Liu X, et al. T helper 17 and T helper 1 cells are increased but regulatory T cells are decreased in subchondral bone marrow microenvironment of patients with rheumatoid arthritis. Am J Transl Res 2016;8(7):2956–68.

[39] Eisenstein EM, Williams CB. The T(reg)/Th17 cell balance: a new paradigm for autoimmunity. Pediatr Res 2009;65(5) Pt 226r-31r.

[40] Giannini D, Antonucci M, Petrelli F, Bilia S, Alunno A, Puxeddu I. One year in review 2020: pathogenesis of rheumatoid arthritis. Clin Exp Rheumatol 2020;38(3):387–97.

[41] Ozgul Ozdemir RB, Soysal Gunduz O, Ozdemir AT, Akgul O. Low levels of pro-resolving lipid mediators lipoxin-A4, resolvin-D1 and resolvin-E1 in patients with rheumatoid arthritis. Immunol Lett 2020;227(8):34–40.

[42] Norling LV, Perretti M. The role of omega-3 derived resolvins in arthritis. Curr Opin Pharmacol 2013;13(3):476–81.

[43] Sugimoto MA, Vago JP, Teixeira MM, Sousa LP. Annexin A1 and the resolution of inflammation: modulation of neutrophil recruitment, apoptosis, and clearance. J Immunol Res 2016;2016(1):1–13.

[44] Fattori V, Amaral FA, Verri WA. Neutrophils and arthritis: role in disease and pharmacological perspectives. Pharmacol Res 2016;112(1):84–98.

[45] Leipe J, Grunke M, Dechant C, Reindl C, Kerzendorf U, Schulze-Koops H, Skapenko A. Role of Th17 cells in human autoimmune arthritis. Arthritis Rheum 2010;62(10):2876–85.

[46] Dominguez-Villar M, Hafler DA. Regulatory T cells in autoimmune disease. Nat Immunol 2018;19(7):665–73.

[47] Lee GR. The balance of Th17 *versus* Treg cells in autoimmunity. Int J Mol Sci 2018;19(3):730.